Active quantum distillation

Muchun Yang and D. L. Zhou [*]

Institute of Physics, Beijing National Laboratory for Condensed Matter Physics, *Chinese Academy of Sciences*, Beijing 100190, China
and School of Physical Sciences, *University of Chinese Academy of Sciences*, Beijing 100049, China

Quantum distillation is a modern technology to decrease the von Neumann entropy of a subsystem by coherent system dynamics. Here we propose an active quantum distillation protocol, in which a bang-bang theme is applied to actively control the coherent dynamics of our system in order to obtain a subsystem with the von Neumann entropy as low as possible. For a bipartite bosonic system, we derive the analytical expression of the entropy lower bound of one subsystem under any unitary transformation for mixed states with conservation of particles. The lower bound is validated by numerical simulations on the Bose-Hubbard model, where the coherent evolution is controlled by tuning one interaction term of the Hamiltonian. Our protocol can be used to decrease the entropy of one subsystem lower than the total bipartite state and increase the number of bosons or only distill out very few bosons in the subsystem.

I. INTRODUCTION

Decreasing the entropy of a quantum system is an essential task in quantum science and technologies. Low entropy states play an important role in the study of quantum many-body physics, such as the quantum phase transition [1,2], topological order states [3,4], and Bose-Einstein condensation [5–7]. To get manifests of those quantum phenomena one must measure some physical quantities on low entropy states. For example, the quantum phase transition is usually accompanied by close of energy gap between their eigenstates, and topological order systems have a topological entanglement entropy on their ground states. Consider a thermal state $\rho = e^{-\beta(H+V)}$ with Hamiltonian $H + V$ and inverse temperature $\beta = 1/T$. If we increase the strength of the potential V, it is equivalent to increase the inverse temperature of the state. A similar idea is also mentioned in quantum virtual cooling [8], which is to square the state to get half of the temperature. Thus the temperature somehow does not capture the essence of the low-energy quantumness. However, as a fundamental quantity in thermodynamics and quantum information, low entropy is the most essential manifestation of the high purity of a quantum state.

In order to get low entropy states, quantum distillation [9–11] technologies are proposed. Quantum distillation refers to a quantum dynamics that makes the final states smaller samples with purer quantum states than initially present. In the case of fermions, numerical simulation shows that during the expansion and with the strongly repulsive interaction, doublons group together and form a low entropy state [10]. In the experiment with a cloud of bosonic atoms trapped in one-dimensional optical lattices [11], some singlons are observed to quantum distill out of the doublon center.

Here, to avoid confusion, we point out that the term "distillation" can also be used for distilling smaller number of

higher quality states, from higher number of copies of states with lower quality, such as entanglement distillation [12–14]. However, as in the relevant literature [9–11], we use the other meaning of "distillation" here, which refers to making the final state purer, regardless of the number of copies.

The advancement of quantum simulation techniques based on cold atom experiments has made it possible to experimentally implement quantum distillation protocols. Controlling the interaction Hamiltonians for Bose-Hubbard models has been achieved on cold atom experiment platforms [15–26]. And experimentalists can measure the entanglement entropy and mutual information in Bose-Hubbard models by using quantum interference of many-body twins to measure second-order Rényi entropy [27]. The boson-related Hamiltonians can also be simulated on a superconducting quantum simulator using a boson-to-qubit mapping [28,29].

Here we aim at getting low entropy states from a thermal mixed state in a bosonic system through quantum distillation. To be exact, we focus on decreasing the entropy of one subsystem lower than the total system without distilling out many bosons from this subsystem. Previous quantum distillation protocols were based on the expansion from a confined region pure state to another empty lattice. In the final state, the region where doublons group together has entropy nearly equal to zero [10]. For an initial pure state, the entropy of the final target state will be never less than the total state. In this paper we propose *active quantum distillation*, which is a precise quantum control protocol to decrease the von Neumann entropy without distilling out many bosons. For a bipartite bosonic mixed state AB, we derive the analytical expression of the entropy lower bound of subsystem B under a unitary transformation U_{AB}. We then construct a unitary evolution by only controlling the interaction Hamiltonian between B and A as illustrated in Fig. 1. The control protocol is constructed by a simple greedy search algorithm.

Our protocol can be used to group bosons together or to distill out some bosons based on different site configurations

---

[*]Contact author: zhoudl72@iphy.ac.cn
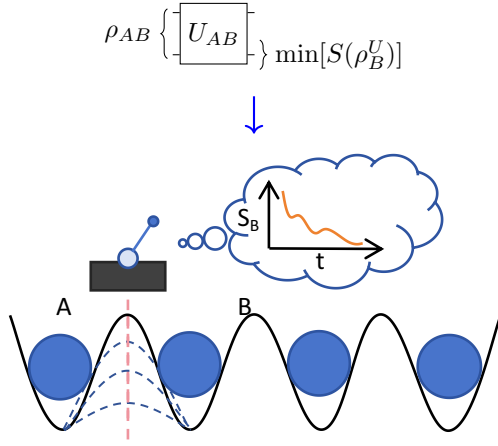
FIG. 1. Active quantum distillation protocol for decreasing the entropy of system B in the Bose-Hubbard model. The strength of the interaction terms in the Hamiltonian is controlled during the time evolution. The total time t_f is divided into N time steps, each of which is δt. The interaction strength can be discretely controlled such that the system will evolve along the direction of decreasing S_B to minimum.

and control parameter choices. In the general case where subsystem A has more than two sites, by choosing appropriate control parameters, we can decrease the entropy of B lower than the entropy of initial total state AB, and increase the number of bosons in B or only distill out very few bosons. If subsystem A has only one site, we group particles together and decrease the entropy of ρ_B to the entropy of ρ_{AB}, which is the lower bound of the entropy of ρ_B under the unitary transformation U_{AB}. The essence of the quantum distillation phenomenon is to get a purer state with more bosons. We explain this quantum distillation phenomenon from the perspective of quantum information theory. Also the protocol stability is tested by numerical simulations.

II. QUANTUM CONTROL MODEL

We consider the one-dimensional Bose-Hubbard model with open boundary condition, whose Hamiltonian

$$\hat{H}_0 = -J \sum_{i}^{L-1} (\hat{b}_i^\dagger \hat{b}_{i+1} + \text{H.c.}) + \frac{U}{2} \sum_{i=1}^{L} \hat{n}_i(\hat{n}_i - 1), \quad (1)$$

where $\hat{b}_i$ ($\hat{b}_i^\dagger$) is the annihilation (creation) operator of the bosonic mode of site i, $\hat{n}_i = \hat{b}_i^\dagger \hat{b}_i$ is the number operator of mode i, J is the hopping strength, and U is the onsite interaction energy between two bosons. Here we adopt a bang-bang control protocol [30,31], which is widely used in quantum control. In the language of bang-bang control protocol, the total Hamiltonian

$$\hat{H}(t) = \hat{H}_0 + \hat{H}_c(t), \quad (2)$$

where the Hamiltonian $\hat{H}_0$ specified by Eq. (1) is called the drift Hamiltonian, and the control Hamiltonian

$$\hat{H}_c(t) = \gamma(t) J (\hat{b}_{l_A}^\dagger \hat{b}_{l_A+1} + \hat{b}_{l_A+1}^\dagger \hat{b}_{l_A}), \quad (3)$$

which plays a role like a switch to adjust the hopping strength between l_Ath and $(l_A + 1)$th sites. Let us divide our system into subsystem A and subsystem B, where subsystem A contains the sites from the first to the l_Ath, and subsystem B contains the remaining sites. Then our central task is to minimize the von Neumann entropy of the subsystem B at a final time t_f by choosing a suitable $\gamma(t)$, which can be formulated as

$$\min_{\gamma(t)} S[\rho_B(t_f)], \quad (4)$$

where $\rho_B(t)$ is the reduced state of $\rho_{AB}(t)$ [$\rho_B(t) = \text{Tr}_A \rho_{AB}(t)$], and the von Neumann entropy $S(\rho) = -\text{Tr} \rho \ln \rho$. Note that the minimal entropy depends on the initial state $\rho_{AB}(0)$. In our protocol, we take the initial state of the whole system $\rho_{AB}(0) = e^{-\beta H_0}/Z$ with the partition function $Z = \text{Tr}(e^{-\beta H_0})$, where $\beta = \frac{1}{k_B T}$, k_B is the Boltzmann constant, and T is the temperature. In most cases, the minimum entropy obtained is smaller than $S[\rho_{AB}(0)]$. We will see in the following sections that, in the task of minimizing the subsystem B entropy, our protocol is nearly equivalent to that capable of applying any global unitary transformations when $l_A = 1$. And for general cases when $l_A > 1$, our protocol has the appropriate capacities to decrease the entropy of B to be less than $S[\rho_{AB}(0)]$ without losing many bosons.

III. ANALYTICAL LOWER BOUND OF SUBSYSTEM ENTROPY

In this section we derive the analytical expression of the lower bound of one subsystem entropy under any unitary transformation. This lower bound is universal for all bosonic systems but not restricted in the Bose-Hubbard model, since in the derivation we only restrict the total particle number to be conserved and all modes are the same after the unitary transformation. In other words, letting $\hat{N}_{AB} = \sum_{i=1}^{L} \hat{n}_i$, in this section we derive the lower bound under any unitary transformation which is generated by a Hamiltonian commuted with $\hat{N}_{AB}$.

Suppose that $\rho_{AB} = \rho_{AB}(0)$ is a bipartite state with total particle number N_{AB}. The number of sites in A is l_A, and the number of sites in B is l_B with $l_A + l_B = L$. We take the occupation number bases $\{|n_1, n_2, \ldots, n_L\rangle\}$, which are defined as $\hat{n}_i|n_1, n_2, \ldots, n_L\rangle = n_i|n_1, n_2, \ldots, n_L\rangle$ and satisfy $\sum_{i=1}^{L} n_i = N_{AB}$. The reduced density operator of A and B is $\rho_A = \text{Tr}_B \rho_{AB}$ and $\rho_B = \text{Tr}_A \rho_{AB}$. The occupation number bases for ρ_A are $\{|n_1, n_2, \ldots, n_{l_A}\rangle_A\}$, and for ρ_B are $\{|n_{l_A+1}, \ldots, n_L\rangle_B\}$. The number operator of A is $\hat{n}_A = \sum_{i=1}^{l_A} \hat{n}_i$, and the number operator of B is $\hat{n}_B = \sum_{i=l_A+1}^{L} \hat{n}_i$. Let $\hat{n}_A|n_1, n_2, \ldots, n_{l_A}\rangle_A = n_A|n_1, n_2, \ldots, n_{l_A}\rangle_A$, and $\hat{n}_B|n_{l_A+1}, \ldots, n_L\rangle_B = n_B|n_{l_A+1}, \ldots, n_L\rangle_B$.

Both ρ_A and ρ_B are block-diagonal matrices, where different blocks have bases corresponding to different n_A and n_B. So we can write $\rho_A = \oplus_{i=0}^{N_{AB}} \rho_{A,i}$ and $\rho_B = \oplus_{i=0}^{N_{AB}} \rho_{B,i}$. The dimension of each $\rho_{A,i}$ is $d_{A,i} = (i + l_A - 1)!/[i!(l_A - 1)!]$, where $i = N_{AB}, \ldots, 1, 0$. And the dimension of each block in ρ_B is $d_{B,i} = (i + l_B - 1)!/[i!(l_B - 1)!]$, where $i = 0, 1, \ldots, N_{AB}$. $d_{A,i}$ and $d_{B,i}$ satisfy $\sum_{i=0}^{N_{AB}} d_{A,i} \times d_{B,N_{AB}-i} = d_{AB}$, where d_{AB} is the dimension of ρ_{AB}.

Note that, for disentangled subsystems A and B, total system AB is a direct sum of the sector labeled by n_A and n_B

(also known as the superselection rule [32]):

$$\rho_A \otimes \rho_B = \bigoplus_{n_A + n_B = N_{AB}} \rho_{n_A, n_B}, \tag{5}$$

where ρ_{n_A, n_B} is a sector whose subsystem A only has bases with n_A and subsystem B only has bases with n_B. There exist unitary transformations that can entangle A and B:

$$U \rho_A \otimes \rho_B U^\dagger = \bigoplus_{n_A + n_B = N_{AB}} \tilde{\rho}_{n_A, n_B}$$
$$+ \{\text{non-block-diagonal elements}\}, \tag{6}$$

where "non-block-diagonal elements" means the entanglement between two subsystems. Denote the Hilbert space of ρ_{n_A, n_B} as $\mathcal{H}_{n_A, n_B}$, and denote system A and B in $\mathcal{H}_{n_A, n_B}$ as $\mathcal{H}_{A, n_A}$ and $\mathcal{H}_{B, n_B}$. In each ρ_{n_A, n_B} the Hilbert space has tensor product structure, i.e., $\mathcal{H}_{n_A, n_B} = \mathcal{H}_{A, n_A} \otimes \mathcal{H}_{B, n_B}$.

Before going into Theorem 1, we omit the non-block-diagonal elements and rearrange the order of the sectors in Eq. (5). The rearranged sectors are

$$\rho_{AB} = \bigoplus_{k=0}^{N_{AB}} \rho_k, \tag{7}$$

such that the dimension of A of each ρ_k is in decreasing order, i.e., $d_{A,k} \geqslant d_{A,k+1}$. For each ρ_k, the dimension of AB is d_k.

Theorem 1. Suppose the eigendecomposition of the bipartite particle number conservation state ρ_{AB}^0 is $\rho_{AB}^0 = \sum_{j=1}^{d_{AB}} p_j |\psi_j\rangle \langle \psi_j|$. We assume these eigenvalues are in decreasing order, i.e., $p_j \geqslant p_{j+1}$. Divide all eigenvalues p_j into N_{AB} groups ϱ_k, $k = 1, 2, \ldots, N_{AB}$. The number of eigenvalues in group ϱ_k is d_k. Denote the lth eigenvalue in the kth sector as $p_{k,l}$. The division satisfies (i) inside the kth group $p_{k,l} \geqslant p_{k,l+1}$ and (ii) for all l and l' in kth and $(k+1)$th groups $p_{k,l} \geqslant p_{k+1,l'}$.

Let

$$q_{k,b} = \sum_{a=1}^{d_{A,k}} p_{k,(b-1)d_{A,k}+a}. \tag{8}$$

By performing a unitary operation U on AB, the minimal entropy of the subsystem B is

$$\min_U S[\rho_B(U)] = -\sum_k \sum_b q_{k,b} \log_2 q_{k,b}. \tag{9}$$

In particular, if A only has one site, then the dimension of ρ_B equals to the dimension of ρ_{AB}^0, $d_B = d_{AB}$. In this case the optimal U satisfies $\rho_{AB}(U) = \rho_B(U)$, and the condition (i) and (ii) can be ignored. Thus $\min_U S[\rho_B(U)] = S(\rho_{AB}^0)$.

Proof. The lemma we mainly use is for the majorization and von Neumann entropy [33]: Suppose ρ and σ are density operators such that $\rho \prec \sigma$, then $S(\rho) \geqslant S(\sigma)$. For two quantum state density operators ρ and σ, $\rho \prec \sigma$ if and only if $\lambda_\rho \prec \lambda_\sigma$, where $\lambda_{\rho(\sigma)}$ is the list of eigenvalues for operator $\rho(\sigma)$. The majorization between two real vectors $\vec{a} \prec \vec{b}$ with dimension D is defined as (i) $\sum_{i=1}^d a_i \leqslant \sum_{i=1}^d b_i$, $1 \leqslant d \leqslant D$, and (ii) $\sum_{i=1}^D a_i = \sum_{i=1}^D b_i = 1$.

For the case that A only has one site, $l_A = 1$, and $d_B = d_{AB}$. The trace operation actually drops out those non-block-diagonal elements in ρ_{AB}, i.e., $\rho_B = \rho_{AB} - \{\text{non-block-diagonal elements}\}$. When U satisfies $\rho_{AB} = \rho_B$, non-block-diagonal elements are zeros. If $\rho_B \neq \rho_{AB}$,

ρ_{AB} has nonzero non-block-diagonal elements. There exists a block-diagonal unitary matrix U_D that can diagonalize ρ_B, $U_D \rho_{AB} U_D^\dagger = \text{diag}\{\lambda_B\}$, where $\text{diag}\{\lambda_B\}$ represents a diagonal matrix with diagonal elements being the eigenvalues of B. Note that $U_D \rho_{AB} U_D^\dagger = \text{diag}\{\lambda_B\} + \{\text{non-block-diagonal elements}\}$. By the Schur-Horn theorem, $\lambda_{AB} \succ \lambda_B$, therefore $S(B) \geqslant S(AB)$.

For general cases that the site number of subsystem A is larger than 1, $l_A > 1$, and $d_B < d_{AB}$. We aim to show $\rho_B \prec \rho_B^*$, where ρ_B^* is the optimal state of B in Theorem 1, and ρ_B is any other state different from ρ_B^*. From the above situation we learn that the non-block-diagonal elements will increase the entropy of one subsystem, so in the following we will only consider the density operator being block diagonal, and only focus on any one of the sectors. We first note that if the sector in ρ_{AB} is not diagonal, there exists a doubly stochastic matrix D, such that $\lambda_{\rho_B} = D \times \lambda_{\rho_B^*}$. And this will make $\lambda_{\rho_B} \prec \lambda_{\rho_B^*}$ and leads to a greater entropy of B. We next note that inside one diagonal sector, each eigenvalue of ρ_B in sector ρ_k is obtained from sum of $d_{A,k}$ eigenvalues in ρ_k. So we want to arrange the largest $d_{A,k}$ eigenvalues of ρ_{AB} into the sector with largest $d_{A,k}$, and so on, until the smallest $d_{A,k}$ eigenvalues of ρ_{AB} for the sector with smallest $d_{A,k}$. Any other order of the $\lambda_{\rho_{AB}}$ in ρ_{AB} leads to $\lambda_{\rho_B} \prec \lambda_{\rho_B^*}$.

The full proof in detail is given in Appendix A. ∎

IV. NUMERICAL RESULTS

The total evolution time t_f is divided into N identical time steps $\delta t = t_f / N$. In the jth time step, $(j-1) \times \delta t < t < j \times \delta t$, the control parameter $\gamma_j^{(k)}$ ($k = 1, \ldots, d$) is selected from $\mathcal{C}(\gamma)$, which is a set of d possible choices. Thus $H_j^{(k)} = H_0 + H_c(\gamma_j^{(k)})$ and $U_j^{(k)} = e^{-i H_j^{(k)} \delta t}$. The selected N control parameters construct a path $\Gamma = \{\gamma_1^{(k_1)}, \gamma_2^{(k_2)}, \ldots, \gamma_N^{(k_N)}\}$. The total unitary transformation is $U = \prod_{j=0}^N U_j$.

We use a greedy algorithm to find the control parameters path. For an initial state ρ_0, at the beginning of time step t_j, the state is $\rho_{j-1} = \prod_{i=0}^{j-1} U_i \times \rho_0$. We choose the control parameter in t_j to be

$$\gamma(t_j) = \underset{\gamma_j^{(k)}}{\operatorname{argmin}} S(\rho_{B,j}^{(k)}), \tag{10}$$

where $\rho_j^{(k)} = U_j^{(k)} \times \rho_{j-1}$, and $\rho_{B,j}^{(k)} = \text{tr}_A \rho_j^{(k)}$. If $S(\rho_{B,j}^{(1)}) = S(\rho_{B,j}^{(2)}) = \cdots = S(\rho_{B,j}^{(d)})$, then we choose

$$\gamma(t_j) = \underset{\gamma_j^k}{\operatorname{argmax}} \gamma_j^k. \tag{11}$$

In the following numerical simulations, we choose $\mathcal{C}(\gamma) = \{1, 0.9, 0.8, \ldots, 0.1, 0\}$. In actual numerical simulation we first choose the value of δt, and the value of t_f is chosen to make $S(\rho_B)$ converge to its minimum.

In the case where A only has one site, we show that our active quantum distillation groups particles together and decreases the entropy of ρ_B to the entropy of ρ_{AB}, which is the lower bound of the entropy of ρ_B under arbitrary unitary transformation. From Theorem 1, if A only has one site, the optimal U satisfies $\rho_{AB} = U \rho_{AB}^0 U^\dagger = \rho_B$, and $\min_U S[\rho_B(U)] = S(\rho_{AB})$.
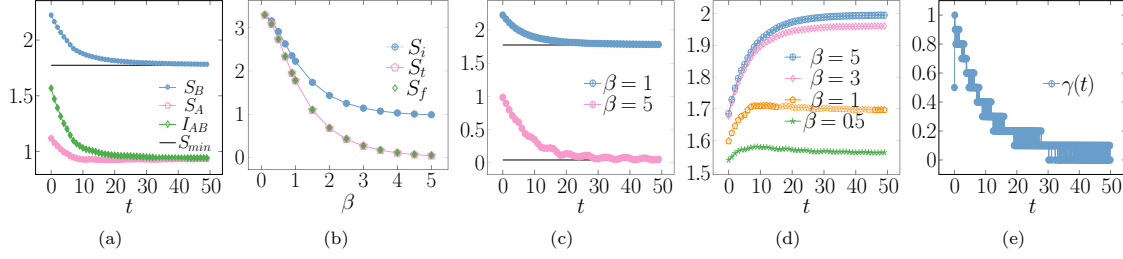
FIG. 2. The numerical results on the Bose-Hubbard model: $L = 4$, $l_A = 1$, $N = 2$, $J = U = 1$. (a) The entropy of subsystem B as the function of time t. $\beta = 1$, $\delta t = 0.1$. (b) The final entropy of subsystem B as a function of β, with other parameters fixed. S_i is the entropy of initial state ρ_B, and S_t is the entropy theoretical lower bound of ρ_B. (c) The entropy of subsystem B as the function of time t for $\beta = 1$ and 5; the control parameters are identified on the model with $\beta = 1$ and are tested on the model with $\beta = 5$. (d) The number of bosons $\langle \hat{n}_B \rangle$ in subsystem B as the function of time t for different β. (e) The choice of γ as the function of t. The path of the $\gamma(t)$ tends to be an adiabatic evolution. The units on the y axis of (a)–(c) are bits; the unit of t and β is J^{-1}.

The entropy of subsystem B as the functions of t is presented in Fig. 2(a). The entropy of B decreases to nearly exactly the theoretical lower bound in $t_f = 30$. The entropy of A and mutual information I_{AB} also decrease under the evolution. The purity of B, which is defined as $P_B = \text{tr}\rho_B^2$, increases under the evolution. In Table I, we list the difference between the final entropy of ρ_B and theoretical lower bound, as well as total evolution time for different size of system. The total evolution time t_f for S_B to converge to the minimum is not scaling with the system size. Actually, the total time t_f depends on the δt. Also the entropy of ρ_B does not converge to the lower bound with any δt. Thus finding the best δt needs a fine-tuning process.

In Fig. 2(b) we plot the final entropy of subsystem B, $S[\rho_B(t_f)]$, as the function of temperature β, with other parameters fixed. The distillation protocol performs well at all temperatures. When the temperature is high, the theoretical lower bound is very close to the initial entropy of ρ_B. However, at low temperature the initial state is more like a pure state, thus subsystem B can be distilled to nearly zero entropy.

The control parameters path we found based on one state with reverse temperature β also works well for other state with β', while other parameters J and U are fixed. The test of the path for the state with $\beta = 1$ on the state with $\beta = 5$ is plotted in Fig. 2(c). We find the control parameters path Γ using the initial thermal state with $\beta = 1$ and use the same path Γ to test the distillation on a thermal state with $\beta = 5$. Under the control parameters path for the state with $\beta = 1$, the entropy of ρ_B with $\beta = 5$ also converges to its lower bound with only a little fluctuation. Other stability tests are shown in Appendix B.

TABLE I. The difference between final entropy and theoretical lower bound, and total evolution time t_f for different size of Bose-Hubbard models with $l_A = 1$. From the table we can see that the total time and errors are parameter dependent. The total time t_f is relatively scaling with $O(1)$ but not scaling exponentially.

Parameter	Value					
(N_{AB}, L)	(1,3)	(2,3)	(3,3)	(2,4)	(3,4)	(4,4)
Difference	0.016	0.055	0.039	0.022	0.034	0.069
t_f	20	100	30	30	50	40

A key hallmark of quantum distillation is the final state with lower entropy and a greater number of bosons. Figure 2(d) shows the number of particles in subsystem B as a function of t for different β. The final state ρ_B groups more bosons with low entropy. When the initial state tends to be a pure state, the final state ρ_B tends to group all the bosons in the initial state ρ_{AB}. In the case that the subsystem A has only one site, the distillation process mainly eliminates the non-block-diagonal elements in the density matrix of ρ_{AB} such that $\rho_{AB} = \rho_B$. Note that

$$\hat{n}_B = \sum_{i=l_A+1}^{L} \hat{n}_i = \oplus_{k=0}^{N_{AB}} k I_{d_{B,k} \times d_{B,k}}, \tag{12}$$

where $k I_{d_{B,k} \times d_{B,k}}$ is an identity matrix with dimension $d_{B,k} \times d_{B,k}$. The largest eigenvalues of ρ_B are mainly distributed on the bases with largest occupation number n_B. The presence of non-block-diagonal elements will diminish the degree of majorization of the diagonal elements of ρ_B, thus causing $\langle \hat{n}_B \rangle$ to be smaller. So we get the conclusion that the distillation process will increase the particle number of subsystem B, which is consistent with numerical simulation plotted in Fig. 2(d).

The control parameters path in our protocol is actually an approximately adiabatic evolution. Figure 2(e) shows $\gamma(t)$ as the function of t. If we add the number of choices d in Γ, the parameter $\gamma(t)$ tends to change continuously. The strength of interaction terms in the Hamiltonian can be tuned adiabatically instead of discretely choosing from Γ.

From Theorem 1, we can decrease the entropy of ρ_B lower than that of ρ_{AB} only when A has more than one site. It is important that in this case we can also group bosons together with $S[\rho_B(U)] = S(\rho_{AB})$ by using some control parameters. However, by fine tuning the control parameters, we can actually find a control path such that $S[\rho_B(U)] < S(\rho_{AB}^0)$ with increasing the number of bosons or only distilling out very few bosons. Combining Theorem 1 and Eq. (12), we get a corollary that when subsystem ρ_B has lowest entropy, the smallest particle number of ρ_B is $\langle \hat{n}_B \rangle = \sum_k k \sum_b q_{k,b}$, which is very close to zero. However, we do not want to get a low entropy state with nearly no bosons. It is important to find a balance between the lower entropy and larger number of particles. Fortunately, the unitary transformation constructed by our protocol does not possess strong abilities to completely
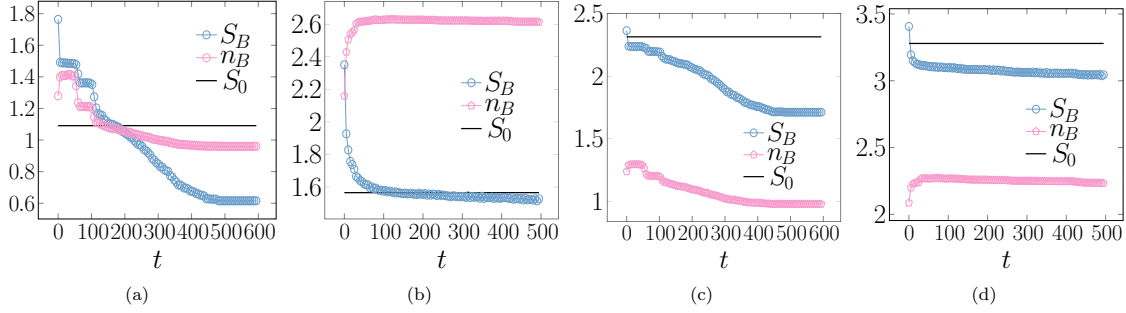
FIG. 3. (a), (b) The entropy and bosons number of system B as the function of t. (a) $L=5$, $l_A=2$, $N=2$, $\delta t=0.6$. (b) $L=6$, $l_A=2$, $N=3$, $\delta t=0.5$. The parameters in the Bose-Hubbard model are $J=U=1$, $\beta=2$. (c), (d) Test of the control parameters path identified in (a) and (b) on the states with $\beta=1$. S_0 is the entropy of the total state ρ_{AB}. $S_{\min}$ is the theoretical lower bound of $S[\rho_B(t_f)]$. $S_{\min}$ is (a) 0.219, (b) 1.067, (c) 0.347, and (d) 1.738. The unit of entropy on the y axis is bits; the unit of t is J^{-1}.

rearrange all the eigenvalues of ρ_{AB} to get the lowest entropy state. In Figs. 3(a) and 3(b), we plot the entropy of ρ_B as the function of t, for states with two sites in A. The control parameters path is searched using Eqs. (10) and (11). For the Bose-Hubbard model with $L=5$, $l_A=2$, and $N=2$, the entropy of ρ_B decreases to half of ρ_{AB} and the bosons number of ρ_B slightly decreases to to around $N/2$. For the Bose-Hubbard model with $L=6$, $l_A=2$, and $N=3$, the entropy of ρ_B decreases to slightly lower than that of ρ_{AB} and the bosons number of ρ_B increases to around $5N/6$. The test of the control parameters path identified in the states with $\beta=2$ on the states with $\beta=1$ is plotted in Figs. 3(c) and 3(d).

It is worth noting that we can also use purity as the target function in Eq. (10), where the purity is defined as $P(\rho)=\mathrm{tr}(\rho^2)$. The active quantum distillation protocol based on optimization of purity can also decrease the von Neumann entropy to its minimum. The performance is basically the same as the protocol based on von Neumann entropy. In Appendix C, we give numerical results about the protocol based on optimization of purity.

V. SUMMARY AND OUTLOOK

We introduce the active quantum distillation protocol to decrease the von Neumann entropy without losing many bosons of the target system by a controlled unitary evolution in a Bose-Hubbard model. Our protocol only needs to control the interaction terms in the Hamiltonian between the two subsystem. We derive the analytical lower bound of the target system entropy, which can be naturally generalized to other bosonic or fermionic models. When one subsystem A only has one site, our protocol can decrease the entropy of the other subsystem B to the entropy of the total state and group particles together at the end of the evolution, where the entropy of the total state is the lower bound of the subsystem entropy. When one subsystem A has more than one site, our protocol can decrease the entropy of the other subsystem B lower than the total system with increasing the number of bosons or only distilling out very few bosons in B. We also find that one control parameter path identified for one set of model parameters can be used in all models with different parameters. The active quantum distillation protocol is actually universal in the whole model parameter space.

In our previous paper [34] about the disentanglement using a quantum circuit, the theoretical lower bound of one subsystem entropy in a spin (qubit) system was given. We show in Appendix D that our entropy minimization protocol is also feasible in qubit systems. Actually, we believe that our minimization protocol is universal for a wide range of states of local Hamiltonians, and will have wide applications in quantum distillation, cooling [35–43], and metrology [44–48] technologies.

APPENDIX A: PROOF OF THEOREM 1

In this section we prove Theorem 1 in the main text. We will first give one definition and three lemmas in matrix theory [49] for the proof of Theorem 1.

Definition 1. A $n \times n$ matrix $A=(a_{ij})$ is called doubly stochastic if

$$a_{ij} \geqslant 0, \qquad \text{for all } i,j, \tag{A1}$$

$$\sum_{i=1}^{n} a_{ij}=1, \quad \text{for all } j, \tag{A2}$$

$$\sum_{j=1}^{n} a_{ij}=1, \quad \text{for all } i. \tag{A3}$$

Lemma 1 (Schur's theorem). Let A be a Hermitian matrix, let diag$\{A\}$ denote the vector whose coordinates are the diagonal entries of A, and let $\lambda\{A\}$ denote the vector whose coordinates are the eigenvalues of A, then diag$\{A\} \prec \lambda\{A\}$.

Lemma 2. Let x and y be n-dimensional vectors, then the following two conditions are equivalent:

(i) $x \prec y$. $\tag{A4}$

(ii) $\mathrm{Tr}\varphi(x) \leqslant \mathrm{Tr}\varphi(y)$ for all convex functions φ from $\mathbb{R}$ to $\mathbb{R}$. $\tag{A5}$

Lemma 3. A matrix A is *doubly stochastic* if and only if $Ax \prec x$ for all vectors x.

Proof. We begin the proof from the case that A only has one site. In this case $d_B = d_{AB}$, and the trace process actually drop out those non-block-diagonal elements, i.e., $\rho_B = \rho_{AB} - \{\text{non-block-diagonal elements}\}$. When U satisfies $\rho_{AB} = \rho_B$, non-block-diagonal elements are zeros, and $\rho_B = \rho_{AB}$. If $\rho_B \neq \rho_{AB}$, ρ_{AB} has nonzero non-block-diagonal elements. There exists a block-diagonal unitary matrix U_D that can diagonalize ρ_B, $U_D \rho_B U_D^\dagger = \text{diag}\{\lambda(B)\}$, where $\text{diag}\{\lambda(B)\}$ represents a diagonal matrix with diagonal elements being the eigenvalues of B. Note that $U_D \rho_{AB} U_D^\dagger = \text{diag}\{\lambda(B)\} + \{\text{non-block-diagonal elements}\}$. By Lemma 1, $\lambda(AB) \succ \lambda(B)$. And according to Lemma 2, $S(B) \leqslant S(AB)$.

We next prove general cases. Denote the optimal unitary transformation as $V = V_1 V_D$, where V_D is a unitary transformation that block diagonalizes ρ_{AB}^0, and $V_1 = \oplus_k V_{1,k}$ is a unitary transformation that diagonalizes $\rho_{AB}^D = V_D \rho_{AB}^0 V_D^\dagger$. Take the bases of $\mathcal{H}_{A,k}$ as $\{|a_k\rangle, 1 \leqslant a_k \leqslant d_{A,k}\}$, and the bases of $\mathcal{H}_{B,k}$ as $\{|b_k\rangle, 1 \leqslant b_k \leqslant d_{B,k}\}$. Let the block-diagonal density matrix be $\rho_{AB}^{\text{BD}} = \oplus_k \rho_k$, and $\rho_k = \sum_{l=1}^{d_{A,k}d_{B,k}} p_{k,l}|\psi_{k,l}\rangle\langle\psi_{k,l}|$. So $V_{1,k}|\psi_{k,(b-1)d_k^A+a}\rangle = |a,b\rangle_k$. Then

$$\rho_{B,k} = \sum_{a,b} p_{k,(b-1)d_{A,k}+a}\text{Tr}_A(|\psi_{k,(b-1)d_{A,k}+a}\rangle\langle\psi_{k,(b-1)d_{A,k}+a}|)$$
$$= \sum_b q_{k,b}|b\rangle\langle b|_k, \tag{A6}$$

where

$$q_{k,b} = \sum_{a=1}^{d_{A,k}} p_{k,(b-1)d_{A,k}+a} \tag{A7}$$

which implies $S(\rho_B(V)) = -\sum_k \sum_b q_{k,b} \log_2 q_{k,b}$.

(1) If $\rho_{AB} = U\rho_{AB}^0 U^\dagger$ is not diagonal but block diagonal, $U = U_D V_1 V_D$, where U_D is a block-diagonal unitary matrix. And $U_D = \oplus_k U_{D,k}$, where $U_{D,k}$ is a unitary matrix in kth subspace. The eigendecomposition of $\rho_{B,k}(U)$ is

$$\rho_{B,k}(U) = \sum_b q_{k,b}(U)|b(U)\rangle\langle b(U)|_k, \tag{A8}$$

and

$$\rho_{B,k}(U) = \rho_{B,k}(U_{D,k}V_{1,k})$$
$$= \sum_{a,b} p_{k,(b-1)d_k^A+a}\text{Tr}_A(U_{D,k}|a,b\rangle\langle a,b|U_{D,k}^\dagger)$$
$$= \sum_{m,n} \sum_{a,b} p_{k,(b-1)d_k^A+a}\langle m,n^{(U)}|_k U_{D,k}|a,b\rangle\langle a,b|_k$$
$$\times U_{D,k}^\dagger|m,n^{(U)}\rangle|n^{(U)}\rangle\langle n^{(U)}|_k$$
$$= \sum_{m,n} p_{(k),m,n}^{(U)}|n^{(U)}\rangle\langle n^{(U)}|_k, \tag{A9}$$

where

$$p_{(k),m,n}^{(U)} = \sum_{a,b} B_{m,n;a,b}^{(k)} p_{(k),(b-1)d_{A,k}+a} \tag{A10}$$

with

$$B_{m,n;a,b}^{(k)} = \langle m,n^{(U)}|_k U_{D,k}|a,b\rangle_k\langle a,b|_k U_{D,k}^\dagger|m,n^{(U)}\rangle_k. \tag{A11}$$

Combining Eqs. (A8) and (A9), we arrive at

$$q_{k,b}(U) = \sum_n p_{k,b,n}^{(U)}. \tag{A12}$$

Note that $B_{m,n;a,b}^{(k)} \geqslant 0$, and $\sum_{a,b} B_{m,n;a,b}^{(k)} = \sum_{m,n} B_{m,n;a,b}^{(k)} = 1$, namely, B is a doubly stochastic matrix. According to Lemma 3, we obtain

$$p_k^{(U)} \prec p_k. \tag{A13}$$

Now we denote $p_{k,\downarrow}^{(U)}$ as $p_k^{(U)}$ in decreasing order. Similarly, we introduce $q_{k,\downarrow,b}^{(U)} = \sum_a p_{\downarrow,k,(b-1)d_k^A+a}^{(U)}$. According to the definition of majorization,

$$q_\downarrow^{(U)} \prec q_k, \tag{A14}$$

$$q_k^{(U)} \prec q_{k,\downarrow}^{(U)}, \tag{A15}$$

which implies that $q_k^{(U)} \prec q_k$. According to Lemma 2,

$$S[\rho_A(V)] \leqslant S[\rho_A(U)]. \tag{A16}$$

This completes the first part of the proof.

(2) If ρ_{AB} is not block diagonal, let ρ_{AB}^D be the block-diagonal part of ρ_{AB}. There exists a U^D, such that $U^D \rho_{AB}^D U^{D\dagger} = \text{diag}\{\lambda(\rho_{AB}^D)\}$. Note that $U^D \rho_{AB} U^{D\dagger} = \text{diag}\{\lambda(\rho_{AB}^D)\} + \{\text{non-block-diagonal elements}\}$. By the Schur-Horn theorem, $\lambda(\rho_{AB}) \succ \lambda(\rho_{AB}^D)$. Then we repeat the proof in step 1, and we finish our proof of step 2.

(3) Our protocol in Theorem 1 is actually as follows: divide the eigenvalues of ρ_{AB}^0 into each subspace, and the larger eigenvalues are in the subspace with larger d_A. When ρ_{AB} is diagonal, each $q_{k,b}$ is the sum of $d_{A,k}$ eigenvalues of ρ_k. So we want the situation in which the larger $d_{A,k}$ the larger $p_{k,l}$. Then by definition of majorization, when ρ_{AB} is diagonal, any order that differs from the above protocol will result in a set $\{q'\}$, such that $q' \prec q$, where q is the set in Eq. (A7). This completes the proof of Theorem 1. ∎

APPENDIX B: ADDITIONAL NUMERICAL DETAILS

In this section we give additional numerical details about the active quantum distillation protocol. In Figs. 4(a)–4(d), we plot the final entropy of subsystem B, $S[\rho_B(t_f)]$, as the function of J and U on Bose-Hubbard models with different parameters. When the hopping strength is large, bosons move faster than the small hopping amplitude, therefore larger hopping strength leads to a shorter evolution time. For a model with $N = 2$ and $L = 4$, when the onsite repulsion U is small, the model is in free bosons limit $U \to 0$, and the evolution time becomes longer. Strong onsite repulsion makes the model to be in a hard-core bosons limit $U \to \infty$, and the evolution time becomes longer. However, for a model with unit filling ($N = 4$ and $L = 4$, $N/L = 1$), large U implies fast minimization.

We also numerically show that our protocol is robust under the impact of imperfect timekeeping. The impact of imperfect
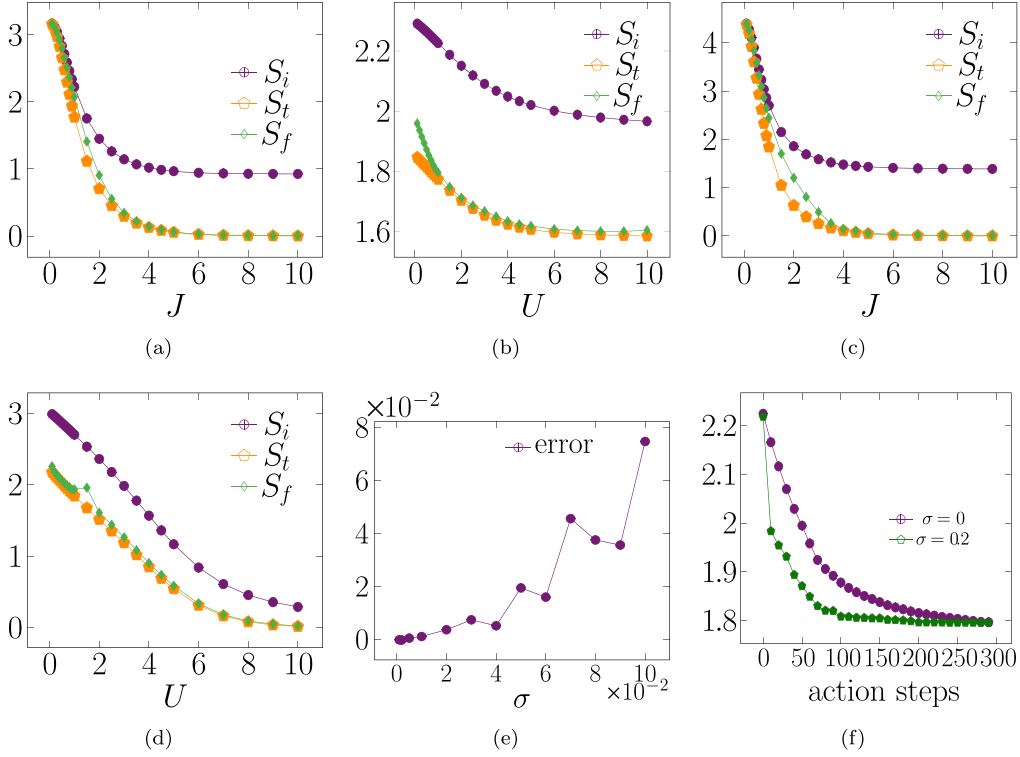
FIG. 4. (a), (b) The final entropy of subsystem B, $S[\rho_B(t_f)]$ as the function of J and U, on the Bose-Hubbard model with $L = 4$, $l_A = 1$, $N = 2$, and $\beta = 1$. S_i is the initial entropy of ρ_B, and S_t is the theoretical lower bound of $S[\rho_B(t_f)]$. (a) The final entropy of subsystem B with different initial-state parameter J, with $U = 1$. The unit of entropy is bits; the unit of J is U^{-1}. (b) The final entropy of subsystem B with different initial-state parameter U, with $J = 1$; the unit of U is J^{-1}. (c), (d) The final entropy of subsystem B, $S[\rho_B(t_f)]$ as the function of J and U, on the Bose-Hubbard model with $L = 4$, $l_A = 1$, $N = 4$, and $\beta = 1$. (c) The final entropy of subsystem B with different initial-state parameter J, with $U = 1$. (d) The final entropy of subsystem B with different initial-state parameter U, with $J = 1$. (e) The relative error of the final entropy with imperfect timekeeping evolution as functions of standard deviation of the timekeeping tick σ for states with $L = 4$, $N = 2$, $dt = 0.1$. The error is defined as the difference between S_f and S_t. (f) The comparison between method with and without random dt. The entropy of subsystem B as the functions of t for the method with the randomness ($\sigma = 0.2$) and without the randomness ($\sigma = 0$) is plotted. The method with randomness converges to the minimum with less steps.

timekeeping on quantum control was shown in [50]: for cooling a qubit with protocol based on a SWAP gate, timekeeping error only impacts the rate of cooling but not the achievable temperature. In a time duration τ, the imperfect timekeeping means the evolution of an initial state ρ is given as

$$\rho' = \int_{-\infty}^{\infty} dt \, \frac{e^{\frac{(t-\tau)^2}{-2\sigma^2}}}{\sqrt{2\pi}\sigma} e^{-iHt} \rho e^{iHt}, \qquad (B1)$$

where σ is the standard deviation of the timekeeping tick distribution. Here we numerically show that our protocol is stable against the imperfect timekeeping from the aspects of entropy minimization. Specifically, we first find the optimal control sequence with perfect timekeeping, then we numerically test our optimal control sequence with a Gaussian-error imperfect timekeeping.

In Fig. 4(e) we show the relative error of the final entropy with imperfect timekeeping evolution as functions of standard deviation of the timekeeping tick σ with dt is 0.1. Our protocol remains valid even when the standard deviation of the timekeeping tick distribution σ equals to dt.

To furthermore shorten the total evolution time, the randomness can be used in this protocol. The time step dt can be chosen as a random Gaussian variable with mean $\langle dt \rangle = dt_0$

and standard deviation σ. And we use the above method to find control parameters in each random time step dt_j. This random time step method does not promise that every path we searched will have a shorter evolution time; however, we find that there is a very high probability that we will search out a better path than the method without randomness. The landscape of the entropy is very complex, taking dt as a random variable to some extent increasing the probability to find a better path with shorter total evolution time. In Fig. 4(f) we show the comparison between the method with random time period and without random time period. The entropy of subsystem B as a function of t for the method with randomness and without randomness is presented.

APPENDIX C: ACTIVE QUANTUM DISTILLATION BASED ON OPTIMIZATION OF PURITY

In this section we give the numerical results of the active quantum distillation protocol based on optimization of purity. We change the target function in the main text,

$$\gamma(t_j) = \underset{\gamma_j^{(k)}}{\operatorname{argmin}} S\big(\rho_{B,j}^{(k)}\big), \qquad (C1)$$
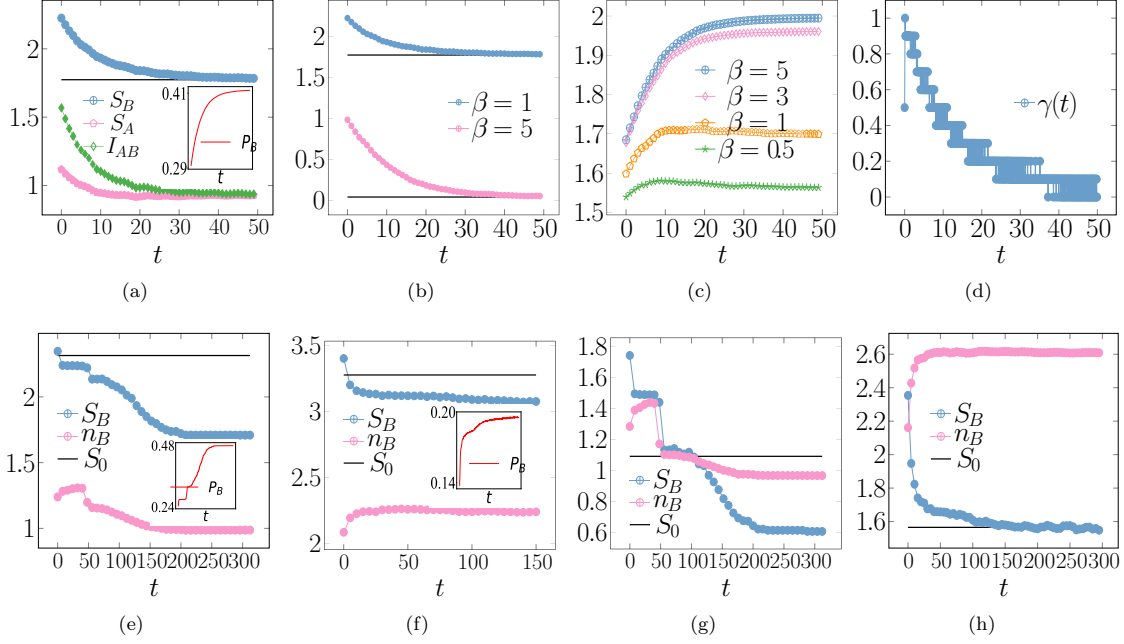
FIG. 5. The numerical results using the purity as the target function. (a) The entropy of subsystem B as the function of time t. $\beta = 1$, $\delta t = 0.1$. Inset: The purity of subsystem B as the function of time t. (b) The entropy of subsystem B as the function of time t for $\beta = 1$ and 5; the control parameters are identified on the model with $\beta = 1$ and are tested on the model with $\beta = 5$. (c) The number of bosons $\langle \hat{n}_B \rangle$ in subsystem B as the function of time t for different β. (d) The choice of γ as the function of t. The path of the $\gamma(t)$ tends to be an adiabatic evolution. (e), (f) The entropy and bosons number of system B as the function of t. (e) $L = 5$, $l_A = 2$, $N = 2$, $\delta t = 0.8$. (f) $L = 6$, $l_A = 2$, $N = 3$, $\delta t = 0.5$, where $\beta = 2$. The parameters in the Bose-Hubbard model are $J = U = 1$, $\beta = 1$. Inset: The purity of subsystem B as the function of time t. (g), (h) Test of the control parameters path identified in (e) and (f) on the states with $\beta = 2$. The unit on the y axis of entropy is bits; the unit of t is J^{-1}.

to the purity of the subsystem B,

$$\gamma(t_j) = \underset{\gamma_j^{(k)}}{\mathrm{argmax}} \, P\big(\rho_{B,j}^{(k)}\big), \tag{C2}$$

where the purity of the subsystem B is defined as

$$P(\rho_B) = \mathrm{tr}\big(\rho_B^2\big). \tag{C3}$$

The numerical results based on optimization of purity are given in Fig. 5. In the case where A has one site, using the purity as the target function is almost the same as using the von Neumann entropy. In the case where A has more than one

site, a slightly different time step δt will be used when using the purity as the target function.

APPENDIX D: ENTROPY MINIMIZATION PROTOCOL FOR THE TRANSVERSE FIELD ISING MODEL

In this section we show some numerical results about our entropy minimization protocol in the spin (qubit) system. In our previous paper [34], the theoretical lower bound of one subsystem entropy in the spin (qubit) system was given. For a bipartite state ρ_{AB}^0 with the eigendecomposition
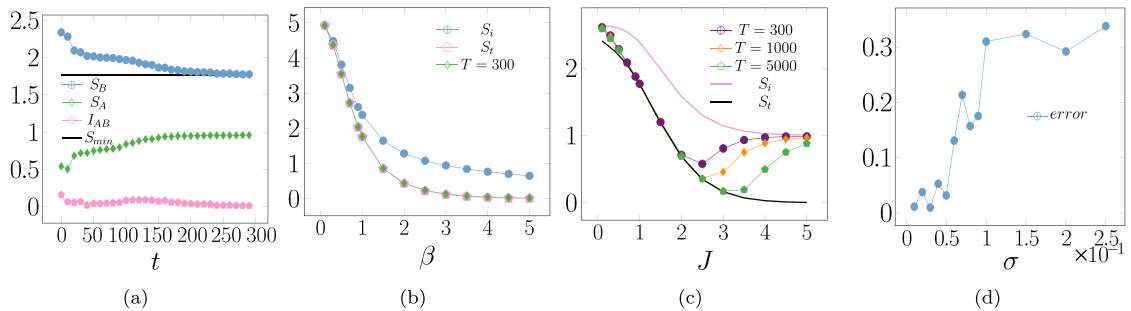
FIG. 6. (a) The entropy of system B of the six-qubit Ising model with $J = 1$ and $\beta = 1$ as functions of the evolution time; the time duration $\delta t = 1$. The unit of the entropy is bits; the unit of t is J^{-1}. (b) The final entropy of B as the function of β for the Ising model with fixed parameter $J = 1$. S_i is the initial entropy of ρ_B, and S_t is the theoretical lower bound of $S[\rho_B(t_f)]$. The unit of β is J^{-1}. (c) The final entropy of B as the function of J for the Ising model with fixed $\beta = 1$. The unit of J is β^{-1}. (d) The relative error of the final entropy with imperfect timekeeping evolution as a function of standard deviation of the timekeeping tick σ for a six-qubit Ising model with $dt = 0.5$. The error is defined as the difference between S_f and S_t.

$\rho_{AB}^0 = \sum_{j=1}^{d_{AB}} p_j |\psi_j\rangle\langle\psi_j|$, assuming these eigenvalues are in decreasing order, by performing a unitary operation U on AB, the minimal entropy of the subsystem B is

$$\min_U S[\rho_B(U)] = -\sum_j p_j \log_2 p_j, \tag{D1}$$

where $q_j = \sum_{a=1}^{d_A} p_{(j-1)d_A+a}$.

Here we show the numerical results of our entropy minimization protocol on the transverse field Ising model, whose Hamiltonian is

$$H_0 = -\sum_{i=1}^{L} J\sigma_i^x \sigma_{i+1}^x - \sigma_i^z, \tag{D2}$$

and the control Hamiltonian is

$$H_c(t) = \gamma(t) J\sigma_{l_A}^x \sigma_{l_A+1}^x. \tag{D3}$$

In Fig. 6(a) we plot the entropy of ρ_A, ρ_B, and the mutual information between A and B, as the function of t. Here we choose $\mathcal{C}(\gamma) = \{1, 0.5, 0.3, 0.2, 0.1, 0\}$, and set $L = 6$, $l_A = 1$. The mutual information between A and B, I_{AB}, first fluctuates, and decreases to nearly zero at around $t = 50$, then increases at around $t = 100$, and finally decreases to zero in the end. We note that the time period of the I_{AB} decreases exactly corresponding to the decreasing of S_A, which indicates that I_{AB} acts as a kind of "potential" to decrease S_B. In the landscape of S_B, I_{AB} decreases to zero corresponding to getting a local minimum of S_B, and the increasing of I_{AB} corresponding to climbing out of the local minimum. The entropy of A reaches the maximum value 1 for A equal to one qubit.

TABLE II. The difference between the final entropy and the theoretical lower bound, and total evolution time t_f for different size of Ising models. The total time and difference are model dependent and parameter dependent. The total time is relatively scaling as $O(1)$ and is not scaling exponentially with N.

Parameter	Value					
N	4	5	6	7	8	10
Difference	0.013	0.092	0.019	0.065	0.047	0.044
t_f	30	500	300	420	500	220

In Figs. 6(b) and 6(c), we plot $S[\rho_B(t_f)]$ as the function of β and J. When the parameter J is relatively big, i.e., the two-body interaction in the Hamiltonian is strong, the evolution time becomes longer. Strong interaction makes the initial ground state tend to be a Greenberger-Horne-Zeilinger state $(|+\rangle^{\otimes L} + |-\rangle^{\otimes L})/\sqrt{2}$, thus the initial state is strongly entangled and the initial I_{AB} is big, which leads to a longer evolution time. When the two-body interaction in the Hamiltonian is very weak, the ground state tends to be a product state $|0\rangle^{\otimes L}$, and the entropy minimization nearly fails. Weak interaction leads to a small I_{AB} of the initial state and a weak ability to increase the I_{AB} during the evolution, thus leading to no such kind of "potential" to decrease S_B.

In Fig. 6(d) we show the relative error of the final entropy with imperfect timekeeping evolution as a function of standard deviation of the timekeeping tick σ with dt is 0.5. Our protocol remains valid when the standard deviation of the timekeeping tick distribution σ is lower than 10% of dt. In Table II, we list the difference between the final entropy of ρ_B and the theoretical lower bound, as well as total evolution time for different size of the system.

[1] S. Sachdev, *Quantum Phase Transitions*, 2nd ed. (Cambridge University Press, New York, 2011).

[2] B. Gadway, Nat. Phys. **18**, 231 (2022).

[3] B. Zeng, X. Chen, D. L. Zhou, X. G. Wen, *Quantum Information Meets Quantum Matter* (Springer, New York, 2019).

[4] A. Kitaev and J. Preskill, Phys. Rev. Lett. **96**, 110404 (2006).

[5] I. Georgescu, Nat. Rev. Phys. **2**, 396 (2020).

[6] A. J. Leggett, Rev. Mod. Phys. **73**, 307 (2001).

[7] M. B. Kim, A. Svidzinsky, G. S. Agarwal, and M. O. Scully, Phys. Rev. A **97**, 013605 (2018).

[8] J. Cotler, S. Choi, A. Lukin, H. Gharibyan, T. Grover, M. E. Tai, M. Rispoli, R. Schittko, P. M. Preiss, A. M. Kaufman, M. Greiner, H. Pichler, and P. Hayden, Phys. Rev. X **9**, 031013 (2019).

[9] T. Porto, Nat. Phys. **11**, 301 (2015).

[10] F. Heidrich-Meisner, S. R. Manmana, M. Rigol, A. Muramatsu, A. E. Feiguin, and E. Dagotto, Phys. Rev. A **80**, 041603(R) (2009).

[11] L. Xia, L. A. Zundel, J. Carrasquilla, A. Reinhard, J. M. Wilson, M. Rigol, and D. S. Weiss, Nat. Phys. **11**, 316 (2015).

[12] C. H. Bennett, G. Brassard, S. Popescu, B. Schumacher, J. A. Smolin, and W. K. Wootters, Phys. Rev. Lett. **76**, 722 (1996).

[13] D. Deutsch, A. Ekert, R. Jozsa, C. Macchiavello, S. Popescu, and A. Sanpera, Phys. Rev. Lett. **77**, 2818 (1996).

[14] S. Ecker, P. Sohr, L. Bulla, M. Huber, M. Bohmann, and R. Ursin, Phys. Rev. Lett. **127**, 040506 (2021).

[15] J. Salfi, J. A. Mol, R. Rahman, G. Klimeck, M. Y. Simmons, L. C. L. Hollenberg, and S. Rogge, Nat. Commun. **7**, 11342 (2016).

[16] C.-C. Chien, S. Peotta, and M. Di Ventra, Nat. Phys. **11**, 998 (2015).

[17] T. Hensgens, T. Fujita, L. Janssen, X. Li, C. J. Van Diepen, C. Reichl, W. Wegscheider, S. Das Sarma, and L. M. K. Vandersypen, Nature (London) **548**, 70 (2017).

[18] F. Schäfer, T. Fukuhara, S. Sugawa, Y. Takasu, and Y. Takahashi, Nat. Rev. Phys. **2**, 411 (2020).

[19] C. Gross and I. Bloch, Science **357**, 995 (2017).

[20] I. Bloch, J. Dalibard, and W. Zwerger, Rev. Mod. Phys. **80**, 885 (2008).

[21] D. Greif, T. Uehlinger, G. Jotzu, L. Tarruell, and T. Esslinger, Science **340**, 1307 (2013).

[22] R. A. Hart, P. M. Duarte, T.-L. Yang, X. Liu, T. Paiva, E. Khatami, R. T. Scalettar, N. Trivedi, D. A. Huse, and R. G. Hulet, Nature (London) **519**, 211 (2015).

[23] K. Winkler, G. Thalhammer, F. Lang, R. Grimm, J. Hecker Denschlag, A. J. Daley, A. Kantian, H. P. Büchler, and P. Zoller, Nature (London) **441**, 853 (2006).

[24] N. Strohmaier, D. Greif, R. Jördens, L. Tarruell, H. Moritz, T. Esslinger, R. Sensarma, D. Pekker, E. Altman, and E. Demler, Phys. Rev. Lett. **104**, 080401 (2010).

[25] J. P. Ronzheimer, M. Schreiber, S. Braun, S. S. Hodgman, S. Langer, I. P. McCulloch, F. Heidrich-Meisner, I. Bloch, and U. Schneider, Phys. Rev. Lett. **110**, 205301 (2013).

[26] U. Schneider, L. Hackermüller, J. P. Ronzheimer, S. Will, S. Braun, T. Best, I. Bloch, E. Demler, S. Mandt, D. Rasch, and A. Rosch, Nat. Phys. **8**, 213 (2012).

[27] R. Islam, R. Ma, P. M. Preiss, M. Eric Tai, A. Lukin, M. Rispoli, and M. Greiner, Nature (London) **528**, 77 (2015).

[28] B. Peng, Y. Su, D. Claudino, K. Kowalski, G. H. Low, and M. Roetteler, arXiv:2307.06580.

[29] X.-H. Deng, C.-Y. Lai, and C.-C. Chien, Phys. Rev. B **93**, 054116 (2016).

[30] Z. An and D. L. Zhou, Europhys. Lett. **126**, 60002 (2019).

[31] Z. An, H.-J. Song, Q.-K. He, and D. L. Zhou, Phys. Rev. A **103**, 012404 (2021).

[32] A. Kitaev, D. Mayers, and J. Preskill, Phys. Rev. A **69**, 052326 (2004).

[33] M. A. Nielsen, Lecture Notes, Department of Physics, University of Queensland, Australia, 2002 (unpublished), p. 53.

[34] Z. An, C. Cao, C.-Q. Xu, and D. L. Zhou, Quantum **8**, 1421 (2024).

[35] P. Taranto, F. Bakhshinezhad, A. Bluhm, R. Silva, N. Friis, M. P. E. Lock, G. Vitagliano, F. C. Binder, T. Debarba, E. Schwarzhans, F. Clivaz, and M. Huber, PRX Quantum **4**, 010332 (2023).

[36] L. del Rio, J. Åberg, R. Renner, O. Dahlsten, and V. Vedral, Nature (London) **474**, 61 (2011).

[37] F. Clivaz, R. Silva, G. Haack, J. B. Brask, N. Brunner, and M. Huber, Phys. Rev. Lett. **123**, 170605 (2019).

[38] R. Silva, G. Manzano, P. Skrzypczyk, and N. Brunner, Phys. Rev. E **94**, 032120 (2016).

[39] T. K. Konar, S. Ghosh, A. K. Pal, and A. Sen(De), Phys. Rev. A **107**, 032602 (2023).

[40] T. K. Konar, S. Ghosh, A. K. Pal, and A. Sen(De), Phys. Rev. A **105**, 022214 (2022).

[41] O. Abah, M. Paternostro, and E. Lutz, Phys. Rev. Res. **2**, 023120 (2020).

[42] M. Lostaglio, D. Jennings, and T. Rudolph, Nat. Commun. **6**, 6383 (2015).

[43] P. Skrzypczyk, A. J. Short, and S. Popescu, Nat. Commun. **5**, 4185 (2014).

[44] V. Giovannetti, S. Lloyd, and L. Maccone, Phys. Rev. Lett. **96**, 010401 (2006).

[45] S. M. Roy and S. L. Braunstein, Phys. Rev. Lett. **100**, 220501 (2008).

[46] Y. Chu, X. Li, and J. Cai, Phys. Rev. Lett. **130**, 170801 (2023).

[47] H. Zhou, J. Choi, S. Choi, R. Landig, A. M. Douglas, J. Isoya, F. Jelezko, S. Onoda, H. Sumiya, P. Cappellaro, H. S. Knowles, H. Park, and M. D. Lukin, Phys. Rev. X **10**, 031003 (2020).

[48] M. Barbieri, PRX Quantum **3**, 010202 (2022).

[49] R. Bhatia, *Matrix Analysis* (Springer, New York, 1997).

[50] J. Xuereb, P. Erker, F. Meier, M. T. Mitchison, and M. Huber, Phys. Rev. Lett. **131**, 160204 (2023).